Радиофизика и радиоастрономия, 2001, т. 6, №1, стр. ??-??

Low-Frequency Carbon Recombination Lines

A. A. Konovalenko, S. V. Stepkin, D. V. Shalunov

Institute of Radio Astronomy of NAS of Ukraine
4 Chervonopraporna St., 61002 Kharkov, Ukraine
E-mail: akonov@ira.kharkov.ua

Received May 17, 2001

The low-frequency carbon recombination lines (with wavelengths up to twenty five and even more meters) became important means of the low-density interstellar plasma diagnostics. An impressive amount of astrophysical information was obtained over the past twenty years – the carbon lines were detected in the frequency range from 12 to 1400 MHz. Correspondingly, the maximum principal quantum numbers of the observed interstellar atoms are more than 800. The medium in the direction of Cassiopeia A is the best studied object, which forms such features. The volume of data for other galactic sources is also increasing. The observation of lines from such highly excited atoms is a unique and effective method for probing the physical conditions of the low-density interstellar plasma as well as the important means for the study of the physics of the high Ridberg state atoms.

1. Introduction

Until the end of 1970's the investigations of the astrophysical phenomenon of radio recombination lines (RRL) were a privilege of the high-frequency radio astronomy. The observations of the hydrogen, helium, carbon, and some other RRLs carried out mainly at the frequencies above 1 GHz (corresponding to the principal quantum numbers $n > 200$) allowed to study various physical and kinematic parameters, such as the temperature, density, size, pressure, and the element abundance of a number of HII regions and their neighborhoods [1]. Naturally, the hydrogen lines turned to be the most informative, because they are formed by the most abundant element. It is ionized mainly by the strong UV radiation ($\lambda < 912$Å) from O and B stars inside the Stromgren zones. The attempts to detect the hydrogen RRLs at the longer wavelengths (up to the metric range) were successful only for some selected objects. The lowest-frequency hydrogen line detected is the $H352\alpha$ feature at 150 MHz, originating in the hot gas located in the direction of the Galactic Center [2]. In spite of that, the importance of the low-frequency RRL investigations became clear many years ago. According to the theoretical estimations [3], rather intensive (due to stimulated emission) low-frequency ($\nu = 100 \div 300$ MHz) hydrogen lines are expected to be formed in cold diffuse ($T_e \sim 100$ K, $N_e \sim 0.03$ cm^{-3}) interstellar components, which are heated and ionized by cosmic and X-rays at the hydrogen ionization rate $\xi_H \sim 10^{-15}$ s^{-1}. Surprisingly, these lines have not been detected yet, indicating that the upper limit of the hydrogen ionization rate is $\xi_H < 10^{-17}$ s^{-1}.

It is important to point out that as early as in 1960's the founder of Ukrainian decametric radio astronomy Professor S. Ya. Braude had proposed to search for the radio recombination lines (with $n > 600$) at the decameter waves. Such a program was started on his initiative, after the radio telescope UTR-2 had been built.

The detection of the spectral features (they turned out to be the RRLs of the strongly excited carbon atoms with $n \sim 630$) in absorption at extremely low frequencies ($\nu < 30$ MHz) [4] with UTR-2 [5, 6] opened new ways of studying the low-density interstellar plasma by means of the

methods of low and very low frequency radio spectroscopy. This brief review is devoted to a description of the most important stages and aspects of these investigations over the past twenty years.

2. General Properties of the Interstellar Medium and the Role of Carbon Atom

2.1. Low-Density Interstellar Plasma

The interstellar medium (ISM) is an important component of galaxies. It is even difficult to enumerate all the significant physical processes in it – a lot of them are really important for our understanding of the Universe. The physical conditions and processes in the ISM are dramatically various, especially for the interstellar gas [7]. Therefore the investigations of the ISM are of a great interest for the astrophysics.

The principal component of the ISM is the gas penetrated by the cosmic rays, magnetic fields, and electromagnetic radiation of all kinds. It is known that the structure of the interstellar gas is complex: the values of the temperature and density (the physical parameters of the first interest) are very different [7]. It is important to note that practically all the gas is ionized, at least at a low rate. Outside the HII regions most part of the gas (completely or partially ionized) has the electron density $N_e < 1$ cm^{-3}. The temperature can be either high ($T_e > 10^3$ K) or low ($T_e < 100$ K). This gas plays a significant role in the energetics, dynamics, and evolution of the galactic matter. As an example, we can mention the first stage of a star birth (the Rayleigh – Taylor instability). It requires the presence of a magnetic field and only a small amount of electrons. One should emphasize that because of the very low emission measure the experimental studies of such a low-density plasma are very difficult in both the spectral lines and continuum.

2.2. Carbon Atoms and the Physical Processes in the ISM

It is believed that most part of the electrons in the neighborhood of the hot interstellar gas is produced by the carbon atoms (this suggestion was first made more than forty years ago). Carbon is the most abundant element ($\mathrm{C/H} = 3.7 \cdot 10^{-4}$) among those having the ionization potential less than that of hydrogen ($E_\mathrm{C} = 11.2$ eV, $E_\mathrm{H} = 13.6$ eV). The UV photons with $912\text{Å} < \lambda < 1100\text{Å}$ arising in the O and B stars and propagating through the medium can ionize carbon almost completely. Cooling of the gas is produced by the emission line corresponding to a fine structure transition of the carbon ions $^2P_{3/2} - {}^2P_{1/2}$ with $\Delta E = 0.0079$ eV, $\Delta T = 92$ K, and $\lambda = 157\mu$. However, an analysis of the heating-cooling equilibrium gives the kinetic temperature T_k of only ~15 K. This is considerably less than the value obtained, for example, from the HI-line observations ($T_k \sim 50 \div 100$ K) [7].

Later on some new factors leading to heating and ionization in the cold components of ISM were proposed, in particular, cosmic rays ($1 \div 2$ MeV) and the X-rays (~10 keV) [8]. This can yield the hydrogen ionization rate $\xi_\mathrm{H} \sim 10^{-15}$ s^{-1} and the electron density $N_e \sim 0.002 \div 0.05$ cm^{-3}. In these models carbon atoms also remain the main cooling element. Note that the expected intensities of the corresponding hydrogen RRLs ($n = 200 \div 400$) would be rather high, but they have not been detected yet. Perhaps, the absence of these lines can be attributed to the almost complete neutrality of hydrogen in the cold components of ISM. Of course, more careful investigations are necessary to clarify the problem.

It is evident that the processes of heating the medium outside the HII region are complicated. In order to summarize the main determining factors, we can mention the photoionization, the cosmic rays, the photoelectric emission of small grains, the magnetic reconnection, the dissipation of the turbulence of the interstellar plasma, and the photoionization of the polycyclic aromatic hydrogen molecules [8-10].

A particular role of carbon as one of the main sources of the electrons and ions in the cold ISM should be stressed especially. The reasons determining the significance of the carbon atom in the ISM are the following:

• carbon is the most abundant element among those having the ionization potential less than that of hydrogen ($\mathrm{C/H} = 3.7 \cdot 10^{-4}$, $E_\mathrm{C} = 11.2$ eV, $E_\mathrm{H} = 13.6$ eV);

• it is almost completely ionized in the diffuse interstellar gas;

• it is the principal element, which determines the cooling and the thermostatic processes in the HI clouds due to the fine structure transition ${}^2P_{3/2} - {}^2P_{1/2}$ with $\lambda = 157$ μ;

• most of the interstellar molecules contain the carbon atoms;

• carbon plays a significant role in the gas-phase chemical reactions and effectively reflects various physical processes in the ISM.

Neutral and ionized carbon can be observed in several ways. Some of them are presented in Fig. 1. The radio astronomical approach, particularly the carbon RRL observations, may be the most promising one.

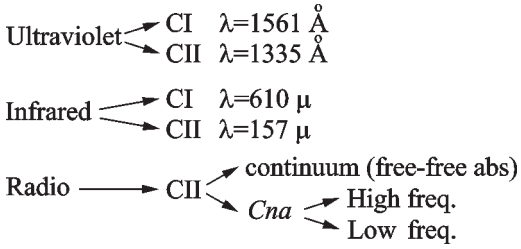

Fig. 1. *Astrophysical methods of observation of the interstellar carbon*

2.3. Carbon RRLs

The first detection of the carbon RRLs was made at high frequencies [11]. After that they were observed in the directions of a number of HII regions [12, 13] simultaneously with the corresponding $Hn\alpha$ lines. As follows from the atomic physics, the mechanism of the carbon line formation is similar to that of the hydrogen lines. The Rydberg's formula gives:

$$\nu_n = cZ^2 R\left(1-\frac{m_e}{M_a}\right)\left(\frac{1}{n^2}-\frac{1}{(n+\Delta n)^2}\right),$$

where c is the velocity of light, Z is the effective nuclear charge, R is the Rydberg's constant, m_e and M_a are the electron and atom masses, n and Δn are the principal quantum number and its increment.

In the case considered only the isotopic shift is present (it is determined by the electron and atom mass ratio), so that the $Cn\alpha$ and $Hn\alpha$ line intensity is determined by the abundances of these elements inside the Stromgren zone. Correspondingly, the carbon lines should be weaker than the hydrogen ones by three orders of magnitude. However, the observed carbon line intensities are much stronger and are comparable to those of the hydrogen features. The carbon lines are believed to arise in the cold ($T_e \sim 100$ K) gas lying at the periphery of HII region. It is the strong dependence of RRL optical depth on the temperature $\left(\tau_L \sim 1/T_e^{2.5}\right)$ that leads to unexpectedly high intensities of the observed carbon features.

Some simple models of the objects, where the carbon RRLs can arise, are presented in Fig. 2.

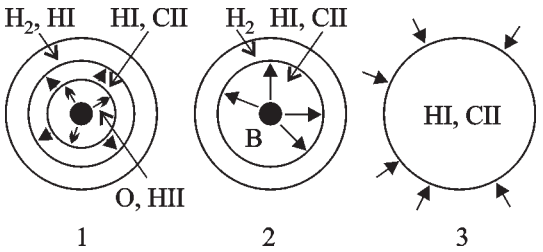

Fig. 2. *Possible ISM objects with ionized carbon (triangular arrows signify the ultraviolet quanta with 912Å < λ < 1100):*
1 – HII regions; 2 – dark dust clouds; 3 – diffuse clouds

It should be stressed that for the objects of type 2 and 3 (those having no $Hn\alpha$ lines) at high frequencies the carbon RRLs were detected only in several selected regions [14]. For the type 3 objects (diffuse CII regions not connected with the HII ones) there is a single detection of $Cn\alpha$ at 1400 MHz [15]. These CII objects are associated with the diffuse HI clouds, which are widespread over the Galaxy.

Fortunately, another way exists, which opens absolutely new opportunities in the RRL studies. It is the radio spectroscopy at low frequencies.

3. Low-Frequency RRLs in the Direction of Cassiopeia A

3.1 Actual Observational Data

The carbon RRLs detected at decameter waves ($\nu < 30$ MHz, $n > 600$) in the direction of Cas A have the following peculiarities:

• they are the first RRLs observed in absorption;

• their intensities are rather high – the integration time necessary for their detection is about one hour;

• line broadening is dramatically strong and surpasses all the examples observed in the astrophysics previously;

• there is an evident variation of the line strength with the frequency;

• association of these lines with rather cold gas in the diffuse CII regions, which are not connected with the HII ones, is a reasonable answer to the question where they arise, because the $Hn\alpha$ lines are not detected in the corresponding directions.

From the Shaver's theory it follows that at higher frequencies such lines should turn into emission [6]. These features were first detected at $\nu > 200$ MHz [16]. The absorption-emission turnover reliably confirms the existence of the stimulated emission in the partially ionized low-density gas lying against a strong continuum radio source. Substantial variation of the line width and intensity, including the change of polarity (such a turnover is not observed at high frequencies), gives an excellent opportunity of diagnostics of the rarefied interstellar plasma. So it is not surprising that the $Cn\alpha$ lines are intensively studied at many radio telescopes, including UTR-2 and RT-70 (Ukraine), GEE-TEE and Ooty (India), DKR-1000 and RT-22 (Russia), Green Bank, the VLA, and Arecibo (USA), Effelsberg (Germany), Parkes (Australia) [17 and references therein].

Cas A is the strongest radio source, against which the RRLs are observed. In this case even for small antennas the antenna temperature sufficiently exceeds that of background. Thus, the same limb projection is investigated in all radio astronomical range, independently of the beam size (Fig. 3). Obviously, this source yields a unique opportunity of the most accurate determination of the line and medium characteristics. So there is no exaggeration in saying that Cas A is the "corner-stone" of the low-frequency radio spectroscopy.

The $Cn\alpha$ lines along the Cas A line of sight have been observed in the very wide frequency range, from 15 MHz ($n \sim 800$) up to 1400 MHz ($n \sim 160$). The total number of the features de-

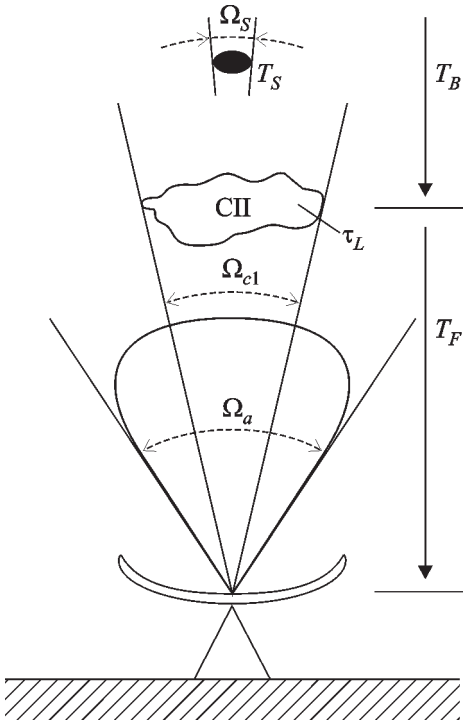

Fig. 3. *Diagram of the low-frequency $Cn\alpha$ line observations.*

$$For\ T_S \gg T_B: \left(\frac{\Delta T_L}{T_C}\right)_{obs} = \left(\frac{\Delta T_L}{T_C}\right)_{real} = -\tau_L;$$

$$for\ T_S \ll T_B: \left(\frac{\Delta T_L}{T_C}\right)_{obs} = \left(\frac{\Delta T_L}{T_C}\right)_{real} \frac{\Omega_{cl}}{\Omega_a} \frac{T_B}{T_B + T_F} \cdot T_S,$$

T_B and T_F are the source, background and frontal medium temperatures, respectively; Ω_s, Ω_{cl} and Ω_a are the source, cloud and antenna solid angles; τ_L is the line optical depth; $\Delta T_L / T_C$ is the line relative intensity; the subscript "obs" means observed

tected comes to several tens. This is an unprecedented achievement in comparison with the other objects studied with RRLs.

Quite recently the lowest frequency spectral lines ($n \sim 812$) were detected near 12 MHz with the radio telescope UTR-2. The atoms with the highest principal quantum numbers of about 860 were observed using the β-lines near 20 MHz at the same instrument (see Fig. 4).

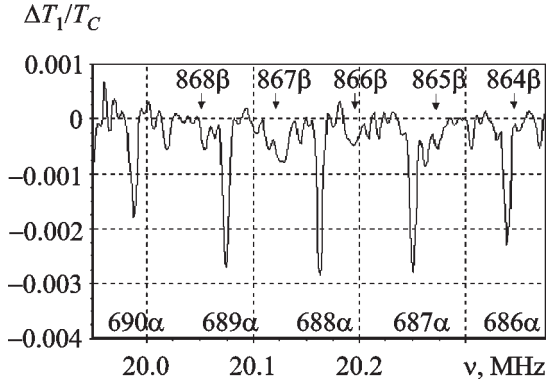

Fig. 4. *A series of carbon RRLs near 20 MHz*

3.2. Problems of Interpretation

The parameters of the low-frequency RRLs are mainly defined by the equations [3] given below in a qualitative form.

The relative intensity is

$$\frac{\Delta T_L}{T_C} = f_1\left(N_e^2, l_p, T_e^{5/2}, \Delta\nu_{LR}, \Delta\nu_{LR}, \Delta\nu_{LD}, b_n, \beta_n\right),$$

the integral relative intensity

$$I_L = \int_{\nu}\left(\frac{\Delta T_L}{T_C}\right)d\nu = f_2\left(N_e^2, l_p, T_e^{5/2}, b_n, \beta_n\right), \quad (1)$$

the pressure broadening

$$\Delta\nu_{LR} \approx f_3\left(N_e^2, T_e^{0.5}, n^{5.2}\right), \quad (2)$$

and the radiative broadening

$$\Delta\nu_{LR} \approx f_4\left(T_R, W, n^{5.8}\right). \quad (3)$$

Here T_e and N_e are the electron temperature and density, l_p is the path length, n is the principal quantum number, T_R and W are the radiation temperature and dilution factor, b_n and β_n are the departure coefficient ($\beta_n = 1 - \frac{kT_e}{h\nu}\frac{d(\ln b_n)}{dn}$, where k and h are the Boltsman and Plank constants).

As is seen from the above equations, the line parameters are strongly dependent on the temperature and density. But the decisive factors are the departure coefficients b_n and β_n, which determine a character of line behavior, including their polarity. The departure coefficients appear to be crucial for model construction. In 1980 it was shown that a mechanism of dielecronic-like recombination due to the fine structure transition $^2P_{3/2} - {}^2P_{1/2}$ ($\Delta T = 92$ K), can considerably modify the departure coefficients of the carbon ion states [18]. Detailed calculations [19] showed that in the case of $T_e \sim 100$ K $b_n\beta_n$ can reach the values of $10 \div 100$. One of other possible mechanisms of $b_n\beta_n$ modification is the underpopulation of the high atomic levels ($b_n \to 0$ with $n \to \infty$) [20, 21]. Let us remind that the classical hydrogenic-like recombination ($b_n \to 1$ with $n \to \infty$) gives the value of $b_n\beta_n$ about 1 for high n [3]. An exotic mechanism of the high-temperature ($T_e > 10^4$ K) dielectronic recombination can provide $b_n\beta_n \sim 10^3$ for the heavy elements [22]. The range where $d l_n b_n / dn$ is negative is of a particular interest: at the lowest frequencies a strong amplification of the absorption lines takes place.

In order to construct a comprehensive physical model of the medium, it is necessary to fit the calculation data obtained using formulas (1)-(3) with the experimental results. Moreover, other astrophysical information on the ISM properties, including, primarily, the data on the HI and molecular lines, the interstellar pressure, and the thermal equilibrium, must be taken into account [21].

At first, two types of the medium models were proposed:

1. The cold gas model with $T_e \sim 20$ K, $N_e \sim 0.3$ cm^{-3}, and the hydrogenic-like level population; CII regions are associated with the cold, clumping, and mainly molecular gas [23].

2. The warm gas model with $T_e \sim 100$ K, $N_e \sim 0.05$ cm^{-3}, and dielectronic-like recombination; the regions of line formation are associated with the diffuse HI clouds and are diffuse themselves [16, 19, 24].

One of the problems met is rather low accuracy of the experimental data, especially at the lowest frequencies ($n > 500$). The difficulty lies not only in the insufficient integration time but also in the very complicated determination of the broad Lorenzian wings of the features. Although some methods of data correction have been proposed [21], the datum accuracy improvement (described below) is of the first importance. In spite of the above mentioned points, on the basis of the already obtained information it can be concluded that the warm gas model better fits to the experimental data.

The anomalous interstellar pressure ($>10^5$ K·cm^{-3}) and rather high value of the observed line width are also among the problems of interpretation, even in the case of optimum fitting of the line parameters to the physical conditions (the electron temperature and density) [21]. So, there is a need for further development and improvement of the models.

3.3. New Physical Models

In the paper [21] a new kind of models was proposed, which involve the mechanism of underpopulation of the high atomic levels. The increase of the derivative provides an agreement between the high line intensity at low frequencies and low intensity at the high ones even if the temperature and density are as low as 35 K and 0.05 cm^{-3}, correspondingly. For this kind of models the $N_H T_e$ factor of about 10^4 K·cm^{-3} becomes reasonable. However the calculated line width at low frequencies is lower than the observed one.

In the paper [17] it was proposed to consider an additional broadening effect (3), caused by the non-thermal radio emission, simultaneously with the decrease of the distance between the line forming region and Cas A supernova remnant. This distance can be about 100 pc, if we take into account the dilution factor and accept the minimum possible, according to observed line widths, full non-thermal radiation temperature (~3200 K at 100 MHz), and the electron density. The best-fit warm gas model parameters are $T_e = 75$ K, $N_e = 0.02$ cm^{-3}, and the emission measure $EM = 0.011$ cm^{-6}·pc [17]. It should be emphasized that the size of the region along the line-of-sight is about 30 pc, that is sufficiently bigger than the linear size of Cas A (~7 pc).

The very important result was obtained while comparing the high-resolution maps of the $C274\alpha$ line distribution across the Cas A limb with the HI and CO data [17]. A better coincidence of the CII regions with the atomic hydrogen distribution is evident. The inhomogeneity of the $C n\alpha$ line forming region is also clear. Probably, a small part of the ionized carbon (as compared to the whole CII region) is spread over the periphery of the molecular clumps [23] and the real medium parameters lie in the intervals $T_e = 35 \div 100$ K and $N_e = 0.01 \div 0.1$ cm^{-3}. The recombination mechanism providing non-hydrogenic level population is always involved. It might be a dielectronic-like process as well. Owing to the observed amplification of absorption features, it is very important as yielding a unique opportunity of plasma diagnostics for a great number of the interstellar objects even when the electron density is less than 0.1 cm^{-3}.

4. Observations of Low-Frequency Carbon RRLs in the Galaxy

4.1. Observational Data for a Number of Galactic Objects

Successful observations of $C n\alpha$ towards Cas A and a fruitful analysis of them motivated the search for such features in the directions to other objects. The galactic background brightness temperature (~30000 K at 25 MHz) always exceeds the electron temperature of an investigated region throughout the Galaxy. However, the values of the observed relative line intensi-

ties (as it is seen in Fig. 3) are less than the real ones due to, in the first turn, the telescope beam dilution and the foreground emission (especially when the objects are distant). So the integration time needed for a reliable detection or the estimation of the upper limits on the line parameters, can reach several hundred hours. In spite of that, the promising perspectives of these investigations are worse all the efforts.

A search for the $C n\alpha$ lines near 25 MHz ($n \sim 640$) in various galactic objects has been carried out over the past two decades with the world largest decameter-wave array UTR-2 [25] and the 128-channel digital correlometer. The effective area of UTR-2 is huge (~150 000 m^2) and the angular resolution is high for a telescope of the decametric range ($\sim 30'$ at 25 MHz) [25]. However, owing to zero spacing problem, which is typical for the T-shaped correlation telescope, and expectedly large spatial sizes of the investigated objects, the North – South arm of UTR-2 (the effective area ~100000 m^2, the beam size $\sim 0.5° \times 12°$) was mainly used in this work. UTR-2 has a well developed and flexible structure that provides convenient ways of sky mapping (for example, there can be five simultaneously operating beams and there is a possibility of array splitting into parts in any configuration) [26]. However, the small number of the correlometer channels restricted the investigation potential. Now a considerable upgrade of the spectral equipment and methods leading to improvement of the sensitivity, the interference immunity, and the reliability of measurements is under way at UTR-2 observatory. In the first turn, it would be very interesting to observe in the directions of the maxima of the HI column density ($N_{\mathrm{H}} > 10^{20}$ cm^{-2}) near the galactic plane (they could be determined, for example, from the HI maps and HI absorption line surveys [27, 28]), the HII regions, SNRs, dark dust clouds and giant molecular clouds. The positive results have been already obtained for many objects, in particular, NGC 2024; $l = 75°$, $b = 0°$; S140; DR-21; L1407; ρ Oph; M16; Per OB2; $l = 35°$, $b = 0°$; $\alpha = 17^{\mathrm{h}}$, $\delta = 70°$.

The relative intensities of the lines obtained are $5 \cdot 10^{-4} \div 1 \cdot 10^{-3}$ and the line widths are $10 \div 50$ km/s. The radial velocities are in a good correspondence with the kinematic parameters of the Galaxy. The estimation of the region sizes across the line-of-sight is rather difficult due to relatively large beam of the North – South telescope arm. A more thorough interpretation is complicated by the absence of reliable data for the higher frequencies ($30 \div 300$ MHz). It is evident that the low-frequency $C n\alpha$ lines arise outside the regions forming the high-frequency ($\nu > 1$ GHz) carbon lines, if any exists.

4.2. Inner Part of the Galaxy

The investigations of the regions along the line-of-sight in the directions close to the Galactic Center have been carried out systematically with the radio telescopes in Parkes at $\nu = 75$ MHz [29], Garibidanur at $\nu = 34.5$ MHz, and Ooty at $\nu = 328$ MHz [30]. Thirty positions with the galactic longitude lying in the interval of $l = 145° \div 342°$ (with the step $5 \div 15°$) were observed at 34.5 MHz. Thirty per cent of these directions gave the $C n\alpha$ line detection. Among other positive results there are the measurements in the directions of $l = 63°$, $l = 75°$ and DR-21 ($l \approx 82°$). The data of the last two observations are in a good agreement with the UTR-2 data. The emission carbon lines at 328 MHz were detected in the galactic longitude range of $l = 392 \div 16.5°$. The investigations of these regions at 75 MHz give positive result too. Not only the absorption $C n\alpha$ lines but also the β and γ ones were detected. The most feasible estimate of the angular size of the regions given in the above mentioned works are in the range of $2 \div 4°$. According to the VLA mapping at 330 MHz for $l = 14°$ and $b = 0°$ (it gave the upper limit of the line intensities rather than detection) the clump sizes are more than $10'$ even in the case when the distribution of CII in these regions is very inhomogeneous.

It is important that the line width does not depend upon n for most of the directions in the frequency range $25 \div 328$ MHz ($\Delta\nu_L = 20 \div 50$ MHz). At the same time, for the Cas A direction $\Delta\nu_L$ changes from 5 to 70 km/s. Possibly, the line width is determined only by the systematical and turbulent gas movements. The supposed upper limit of the electron density is $N_e < 0.3$ cm^{-3}.

4.3. Interpretation of Results

The interpretation of the experimental data is complicated by the fact that a number of physical parameters is unknown. The following combinations of the measured line characteristics and missing information are met when the data are interpreted (the Doppler and radiative broadening are supposed to be known and the medium is supposed to be homogeneous):

1. There are two equations ((1) and (2)) and three unknown values (N_e, T_e, S); the beam width is less than the region size or the gas is projected onto a strong compact radio source (like Cas A if, of course, the cloud sizes are not smaller than its limb). The problem is not resolvable, when there are data only for one observed frequency, even the lowest one with the evident pressure broadening. However, if the measurements are multi-frequency the solution can be found (it is better when $\nu_{\max}/\nu_{\min} = 10 \div 20$) because the third equation appears:

$$b_n \beta_n = f(n, T_e, N_e).$$

2. There is the only case for L1407 [31], when even one low-frequency observational point allows to determine all three physical parameters. If the carbon lines and the continuum free-free absorption arise in the same cold gas (there is no HII region) then the third equation for the continuum optical depth τ_c appears to be:

$$\frac{\Delta T_C}{T_C} = 1 - e^{-\tau_c}.$$

As the low-frequency continuum map exists, it is possible to determine the region size and the beam dilution rate.

3. The sizes of the CII regions for most part of the objects described in subsections 4.1 and 4.2 are unknown. The dependence of beam width upon frequency makes a problem as well. So, even approximate estimation of the region sizes (obtained, for example, by the measurements with the same antennas but using various aperture sizes) is very important [32]. Nevertheless, in some cases it is possible to make significant estimations of $N_{e\max}$, $T_{e\min}$, and $S_{\min}$ even having one frequency of the decametric range [33].

In any case, it is important to use all the accessible astrophysical data for construction of a reliable model (they are, for example, the HI and molecular lines, the continuum thermal and non-thermal radio emission, and the 157μ CII emission line).

Using the measurements at three frequencies for the inner part of the Galaxy as well as the angular size estimation, the most feasible values of the medium properties were found. They are the following: $T_e = 40 \div 100$ K, $N_e = 0.003 \div 0.01$ cm^{-3}, and the path length is more than several parsecs. For the direction of $l = 0°$, $b = 0°$ the data from the papers [34-36] were also used. Thus, the low-frequency $C n\alpha$ lines arise mainly in the diffuse rather warm CII regions associated with the HI gas where the conditions for dielectronic-like process exist.

Probably, the lines at the lowest and higher frequencies ($\nu > 200$ MHz) are formed in the regions with the conditions, which are different to some extent. This follows from a slight distinction in the velocities of the absorption and emission lines in several cases [35].

5. Future Perspectives of Low-Frequency RRL Investigation

5.1. New Instrumentation and Methods

During the last years the interest to the low-frequency radio astronomy has grown considerably. It is caused, in particular, by the new opportunities opened by the low-frequency carbon RRL investigations.

The radio telescope UTR-2 remains the most effective instrument at the frequencies less than 30 MHz. It is characterized by the biggest effective area, the high directivity, the broad operating band, the electronic beam steering, and the multi-beam observation regimes. For the spectral investigations there is no sensitivity limitation due to confusion effect, so that the sensitivity can be much better than for the other operating mode of the UTR-2. The recent upgrade of the preamplifier system has provided the uninterrapted frequency range and a good interference immunity,

which is extremely important for the spectral line observations [37].

Many of the world radio telescopes have undergone substantial upgrade related to the operation at the frequencies above 30 MHz. Furthermore, new highly efficient radio telescopes have arisen. First of all one should mention the GMRT (Giant Meter Radio Telescope, India), which is very suitable for the RRL investigations at $50 \div 1400$ MHz. Without any doubt, the development of low-frequency carbon RRL radio spectroscopy is among scientific motivations for building the giant low-frequency arrays of a new generation.

The progress of modern digital electronics and computer techniques provides effective ways of developing the wide-band (up to several dozens of MHz) and multi-channel (up to many thousands) digital correlometers and spectral processors. Such a new correlometer with the maximum sampling rate of 60 MHz and 4096 channels was installed at the UTR-2 observatory. On the other hand, a 1-bit quantization used in the wide-band correlometers of this kind might lead to problems when strong hindering signals are present. Fortunately, the theoretical evaluation and special experiments have shown that with such devices the low-frequency radio spectroscopy at $\nu < 30$ MHz is quite possible in good many cases.

The frequency distance between the lines rapidly decreases with the wavelength:

$$\Delta\nu \approx \frac{6RcZ^2\Delta n}{n^4} \approx \frac{3\nu}{n}.$$

In the range of $20 \div 30$ MHz there are about 90 α-lines and several hundred of β-lines. Simultaneous observation of such a huge number of features leads to a considerable increase of the measurement sensitivity and the corresponding dramatic decrease of the necessary integration time [38].

The line broadening at the lowest frequencies is very high, and a careful analysis of the Voigt profiles is required. One of the effective ways of profile fitting is based on the well known equation:

$$L(\nu) * G(\nu) = F\left\{\overline{F}\{L(\nu)\} \cdot \overline{F}\{G(\nu)\}\right\},$$

$$\overline{F}\{L(\nu)\} = e^{-\pi\Delta\nu_L\tau}, \qquad \overline{F}\{G(\nu)\} = e^{-\frac{\pi^2\Delta\nu_D^2\tau^2}{4\ln 2}},$$

where "*" denotes the convolution procedure; F, $\overline{F}$ are the direct and back Fourier transforms; $L(\nu)$, $G(\nu)$ are the Lorentzian and Gaussian profiles; $\Delta\nu_L$, $\Delta\nu_D$ are the Lorentzian and Gaussian line widths; τ is the argument of the correlation function (the time delay).

Thus, this method lies in fitting the correlation functions measured by the digital correlometer directly.

5.2. Observational Programs

Although for the Cas A direction the most comprehensive data are obtained, the further development of these studies is not excluded. There are promising ways of the accuracy measurement and the Voight profile fitting improvement, especially at the lowest frequencies. The mapping, as made with the VLA, but at the GMRT frequencies of 50 and 610 MHz, would be also important. Preliminary experiments with the UTR-2 gave the carbon RRL detection outside the Cas A limb (the shift was up to 4°), which corresponded to the more extended region of line formation. So further investigations of this kind, as well as the search for the other radio lines towards Cas A (e. g. NI at 26.13 and 15.67 MHz and NaI at 1770 MHz) at low and high frequencies are of a great interest and importance.

The systematic search and study of the $Cn\alpha$ lines in the direction of the galactic plane at the very low ($\nu < 30$ MHz) and low ($\nu < 330$ MHz) frequencies are also very important. The results and estimations obtained show that the features discussed can be detected in a good many galactic regions with the already existing and coming radio telescopes, if one employs new more sophisticated experimental means and methods. The values of the relative line intensity to be measured are about $10^{-3} \div 10^{-4}$. This sensitivity level provides a possibility to obtain a valuable information about the physical parameters and processes in the ISM.

6. Conclusion

The carbon RRLs at low frequencies have opened new opportunities for the diagnostics of the rarified interstellar plasma and the study of the Rydberg atom physics. Although they are already not exotic, their properties and the conditions in the regions of their formation remain mysterious to a great extent and are still very interesting for investigation. In spite of the numerous difficulties met during the line detection and interpretation, the low-frequency carbon RRLs yield unique information not available with the other astrophysical methods.

Acknowledgments. Many thanks to Professor S. Ya. Braude for his stimulation and support of these investigations, as well as to L. G. Sodin for active participation and discussions. This activity is supported in part by the grants INTAS 96 – 0183, 97 – 1964, and INTAS-CNES 97 – 1450.

References

1. P.A. Shaver, ed. Radio Recombination Lines. Dordrecht, Reidel Publ. Co., 1980, 284 pp.
2. K. R. Anantharamaiah, H. E. Payne, D. Bhatacharya. In: Radio Recombination Lines: 25 Years of Investigations. Eds.: M.A. Gordon, R.L. Sorochenko. Dordrecht, Kluwer Acad. Publ., 1990, pp. 259-263.
3. P. A. Shaver. Pramana. 1975, **5**, No. 1, pp. 1-28.
4. A. A. Konovalenko, L. G. Sodin. Nature. 1980, **283**, No. 5745, pp. 360-361.
5. D. H. Blake, R. M. Crutcher, W. D. Watson. Nature. 1980, **287**, No. 5782, pp. 707-708.
6. A. A. Konovalenko, L. G. Sodin. Nature. 1981, **294**, No. 5837, pp. 135-136.
7. L. Spitzer. Physical Processes in the Interstellar Medium. New York, Wiley, 1978, 318 pp.
8. A. Dalgarno, R. A. McCray. Ann. Rev. A&A. 1972, **10**, No. 2, pp. 375-426.
9. R. J. Reynolds. In: The Physics of the Interstellar and Intergalactic Medium, ASP Conference Series, 80. Eds.: A. Ferrara et al. San Francisco, ASP, 1995, pp. 388-391.
10. L. d'Hendecourt, A. Leger. A&A. 1987, **180**, No. 1, pp. L9-L11.
11. P. Palmer, B. Zuckerman, H. Penfield, A. E. Lilley, P. G. Mezger. Nature. 1967, **215**, No. 5096, pp. 40-41.
12. V. Pankonin, C. M. Walmsley, T. L. Wilson, P. Thomasson. A&A. 1977, **57**, No. 3, pp. 341-349.
13. N. G. Kantharia, K. R. Anantharamaiah, W. M. Goss. ApJ. 1998, **504**, No. 1, pp. 375-389.
14. R. L. Brown. In: Radio Recombination Lines. Ed. P.A. Shaver. Dordrecht, Reidel Publ. Co., 1980, pp. 127-140.
15. R. M. Crutcher. ApJ. 1977, **217**, No. 2, pp. L109-L112.
16. H. E. Payne, K. R. Anantharamaiah, W. C. Erickson. ApJ. 1989, **341**, No. 2, pp. 890-897.
17. N. G. Kantharia, K. R. Anantharamaiah, H. E. Payne. ApJ. 1998, **506**, No. 2, pp. 758-772.
18. W. D. Watson, L. R. Western, R. B. Christensen. ApJ. 1980, **240**, No. 3, pp. 956-961.
19. C. M. Walmsley, W. D. Watson. ApJ. 1982, **260**, No. 1, pp. 317-324.
20. S. A. Gulyaev, S. A. Nefedov. Astron. Nachr. 1989, **310**, No. 2, pp. 403-406.
21. H. E. Payne, K. R. Anantharamaiah, W. C. Erickson. ApJ. 1994, **430**, No. 2, pp. 690-705.
22. P. A. Shaver. A&A. 1976, **46**, No. 1, pp. 127-135.
23. R. L. Sorochenko, C. M. Walmsley. A&A Trans. 1991, **1**, No. 1, pp. 31-46.
24. A. A. Konovalenko. Soviet Astron. Lett. 1984, **10**, No. 11, pp. 846-852.
25. S. Ya. Braude, A. V. Megn, L. G. Sodin. Antennas. 1978, **26**, No. 1, pp. 3-15.
26. A. A. Konovalenko. In: AGU Monograph 119. Washington, AGU, 2000, pp. 311-320.
27. W. B. Burton. A&A Suppl. Ser. 1970, **2**, No. 4, pp. 261-289.
28. V. Radhakrishnan, W. M. Goss, J. D. Murray, J. W. Brooks. ApJ. Suppl. Ser. 1972, **24**, No. 203, pp. 49-72.
29. W. C. Erickson, D. McConnel, K. R. Anantharamaiah. ApJ. 1995, **454**, No. 1, pp. 125-133.
30. D. A. Roshi, K. R. Anantharamaiah. MNRAS. 1997, **292**, No. 1, pp. 63-71.
31. A. A. Golynkin, A. A. Konovalenko. Sov. Astron. J. Lett. 1991, **17**, No. 1, pp. 23-29.
32. A. A. Konovalenko. Sov. Astron. J. Lett. 1984, **10**, No. 12, pp. 912-917.
33. A. A. Golynkin, A. A. Konovalenko. Sov. Astron. J. Lett. 1991, **17**, No. 1, pp. 16-22.
34. A. Pedlar, R. D. Davies, L. Hart, P. A. Shaver. MNRAS. 1978, **182**, No. 2, pp. 473-488.
35. K. R. Anantharamaiah, H. E. Payne, W. C. Erickson. MNRAS. 1988, **235**, No. 1, pp. 151-160.
36. G. T. Smirnov, V. V. Kitaev, R. L. Sorochenko, A. F. Scheglov. In: Pushchino: Annual Session of Sci. Council of ASC, Collection of Reports, 1996, p. 3.
37. E. P. Abranin, Yu. M. Bruk, V. V. Zakharenko, A. A. Konovalenko. Radiophysics and Radioastronomy. 1997, **2**, No. 1, pp. 95-102.
38. A. A. Konovalenko. In: Radio Recombination Lines: 25 Years of Investigations. Eds.: M. A. Gordon, R. L. Sorochenko. Dordrecht, Kluwer Acad. Publ., 1990, pp. 175-188.

Низкочастотные рекомбинационные линии углерода

А. А. Коноваленко, С. В. Степкин, Д. В. Шалунов

Низкочастотные рекомбинационные линии углерода (длины волн до 25 метров и более) стали удобным средством диагностики разреженной межзвездной плазмы. В течение последних 20 лет накоплен большой объем астрофизической информации. Линии углерода удалось обнаружить в диапазоне частот от 12 до 1400 МГц, что соответствует главным квантовым числам межзвездных атомов, превышающим 800. Наиболее полная информация получена для среды в направлении радиоисточника Кассиопея А. Постоянно увеличивается объем данных для других объектов Галактики. Наблюдение спектральных линий столь сильно возбужденных атомов оказалось уникальным и эффективным методом исследования физических свойств разреженной межзвездной плазмы, а также важным средством изучения физики ридберговских атомов.

Низькочастотні рекомбінаційні лінії вуглецю

О. О. Коноваленко, С. В. Степкін, Д. В. Шалунов

Низькочастотні рекомбінаційні лінії вуглецю (довжини хвиль до 25 метрів та більше) стали зручним засобом діагностики розрідженої міжзоряної плазми. Протягом останніх 20 років накопичено великий обсяг астрофізичної інформації. Лінії вуглецю вдалося виявити у діапазоні частот від 12 до 1400 МГц, що відповідає головним квантовим числам міжзоряних атомів, що перевищують 800. Найповнішу інформацію отримано для середовища у напрямку радіоджерела Кассіопея А. Постійно збільшується обсяг даних для інших об'єктів Галактики. Спостереження спектральних ліній високозбуджених атомів виявилося унікальним та ефективним методом дослідження фізичних властивостей розрідженої міжзоряної плазми, а також важливим засобом вивчення фізики рідбергівських атомів.